do not displace coordinated vanadium(V), indicating that V(V) is not bound at the anion binding sites.

Criteria for Observable Sharp ^{51}V NMR Lines in Tightly Bound Systems. The observation of sharp ^{51}V NMR signals in the present study contrasts with earlier work in which the signals of protein-bound vanadate were found to be very broad or even unobservable.[13,22-25] While at the present time our studies do not enable us to predict ^{51}V NMR line widths quantitatively, the following qualitative discussion, in conjunction with the scheme of Figure 12 might serve as a useful guide in the search for other suitable metal-protein systems. In general, the feasibility of ^{51}V NMR in such systems will depend on the location of τ_c with respect to the window of motional correlation times between ω_0^{-1} and ω_{int}^{-1}. This is, to some extent, under the control of the experimenter. Clearly, Figure 8 suggests the use of the highest possible magnetic field strength. On the other hand, the same effect can, in principle, be obtained by increasing τ_c by lowering the temperature, increasing solvent viscosity, or attaching the atom or molecule under study to a large macromolecule. This strategy of deliberately slowing down the reorientational motion in a liquid contrasts sharply with the opposite approach frequently taken in the extreme narrowing limit, where efforts are aimed at decreasing correlation times by either raising the temperature or using low viscosity solvents.

In addition, the feasibility of ^{51}V NMR will depend on the minimum achievable line width within this window, which is essentially a function of the electric gradient tensor at the site of the ^{51}V nucleus and the ^{51}V NMR line width outside of the motional narrowing limit. The latter is usually governed by either the ^{51}V chemical shift anisotropy or (at low fields) second-order quadrupolar perturbations, and thus depends also on the external field strength used. In general, sharp lines are expected for symmetric environments with small quadrupolar coupling constants and chemical shift anisotropies. However, it is clear from the above discussion, that under nonextreme narrowing conditions the external magnetic field strength plays a much more crucial role in balancing the effects of relaxation broadening and static broadening, and thus ^{51}V NMR signals observable at 11.7 T might in certain cases be broadened beyond detectibility at a field strength of 1.4 T or vice versa.

Implications of the Nonextreme Narrowing Condition for Quantitative Spectroscopic Applications. In the present study, the nonextreme narrowing condition results in the benefit of excellent spectroscopic resolution which for most ^{51}V NMR applications is usually not achievable in the extreme narrowing limit. On the other hand, this motional regime impacts certain quantitative spectroscopic aspects of quadrupolar solution-state NMR, which have to be borne in mind in future applications. First, the detection sensitivity is decreased by a factor of 5 (for $I = {}^7/_2$), hence requiring the use of more concentrated solutions. In the case of ^{51}V NMR of proteins we estimate a lower detection limit of 0.05 mM in 10-mm NMR tubes on 11.7-T magnets. Additional complications arise from the flip-angle effect. Future chemical applications will require systematic monitoring of the pulse angle dependence over the entire chemical process to be studied and quantitative accounting for any changes observed in the excitation spectrum. Finally, chemical shifts will have to be viewed with some caution, since dynamic frequency shifts will contribute to the resonance positions measured. The latter can be evaluated by field-dependent measurements and at the maximum available field strength. Notwithstanding these methodological constraints, quadrupolar central transition NMR in the nonextreme narrowing limit is expected to offer many interesting new possibilities in future studies of metal protein interactions.

Acknowledgments. A.B. acknowledges grants from the National Institutes of Health (GM-38130) and the Petroleum Research Fund of the American Chemical Society. A.B. acknowledges helpful discussions with N. D. Chasteen. We also acknowledge helpful discussions with J. P. Yesinowski. Some of the NMR studies were carried out at the Southern California Regional NMR Facility, funded by NSF Grant No. CHE 84-40137.

(45) Rehder, D. *Inorg. Chem.* **1988**, *27*, 4312. See ref 10 herein.

ESR and Optical Study of Electron Transfer between the NO Units of an *N,N'*-Dialkoxyurea Cation Radical

Stephen F. Nelsen,*,† James A. Thompson-Colon,† and Menahem Kaftory‡

Contribution from the S. M. McElvain Laboratories of Organic Chemistry, Department of Chemistry, University of Wisconsin, Madison, Wisconsin 53706, and Department of Chemistry, Technion—Israel Institute of Technology, Haifa 32000, Israel. *Received June 16, 1988*

Abstract: Carbonylbis[3-(2-oxa-3-azabicyclo[2.2.2]octane)] (**3**) has a vIP of 8.20 eV and $E^{\circ\prime}$ of 1.17 V vs saturated calomel electrode (0.1 M n-Bu_4NClO_4/CH_3CN). The X-ray structure of crystalline **3**, which exists in a conformation with one NO group *Z* and the other *E* to the carbonyl group, is reported. **3** gives a cation radical having its "hole" instantaneously localized on one NO unit. Analysis of the low-temperature ESR spectra of $\mathbf{3}^{\bullet+}$ in CH_2Cl_2 for electron transfer between two equivalent sites gave $\Delta G^{\ddagger}_{th}$ near 3.5 kcal/mol between −84 and −30 °C. $\mathbf{3}^{\bullet+}$ exhibits a near-IR charge-transfer band which varies between 1320 nm in $CHCl_3$ and 1260 nm in CH_3CN, and the band energy versus Marcus γ value plot for five solvents is linear, as expected for instantaneous hole localization. Extrapolation of this plot to $\gamma = 0$ gives a value of λ_i of 20.5 kcal/mol, producing a λ_o value of 2.1 kcal/mol in acetonitrile using Hush theory.

The 2-oxa-3-azabicyclo[2.2.2]octyl ring system **1**-R has proven useful for study of electron loss equilibria as the R group is changed. The bicyclic ring system Bredt's rule kinetically protects hydrogen loss α to both heteroatoms of the alkoxyamine unit, and long cation-radical lifetimes are observed even when R is a powerfully electron-withdrawing carbonyl group and electron loss is thermodynamically difficult.[1] A principal conclusion from a study

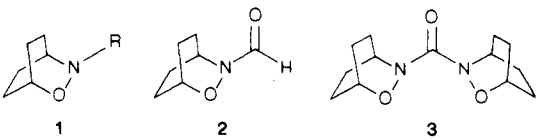

1 **2** **3**

† University of Wisconsin.
‡ Technion—Israel Institute of Technology.

0002-7863/89/1511-2809$01.50/0

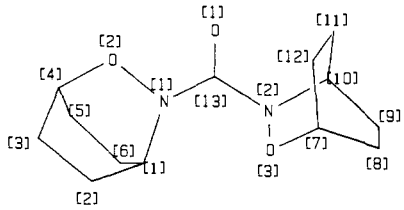

Figure 1. Atom numbering employed for the X-ray crystal structure of **3**.

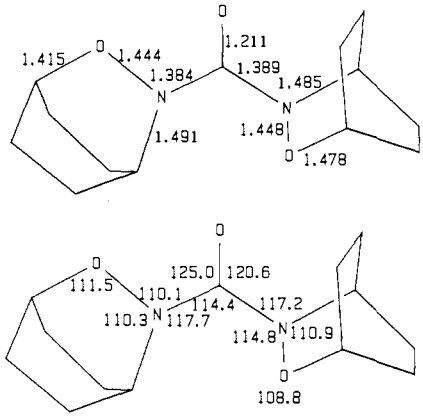

Figure 2. Bond lengths and angles about the heteroatoms for crystalline **3**.

of **1**-R derivatives was that the cation radicals are best described as having a 3e–π NO bond even for acylated compounds like the *N*-formyl derivative **2**.[1] Neutral **2** clearly has strong amide resonance; the nitrogen atom is planar (the average of the bond angles at N, α(av) = 119.8°), the C=O group is aligned with the p orbital at nitrogen (the ON,C=O dihedral angle is 1.5° in crystalline **2**, although the *E* form is more stable in solution), and N,C=O bond rotation is slow on the NMR time scale at room temperature. $\mathbf{2}^{\bullet+}$ was argued from its spin distribution and from calculations to have little N–CO resonance interaction.[1] In this work we consider electron loss from the urea derivative **3**, which has two formally equivalent sites for NO 3e–π bonds in the cation radical. If the above conclusion about bonding in **1**-R cation radicals is correct, the "hole" in $\mathbf{3}^{\bullet+}$ might be localized in one of the bicyclic rings, and the kinetics of electron transfer between them could be considered. We argue that $\mathbf{3}^{\bullet+}$ does exhibit slow electron transfer between its hydroxylamine units and carry out a Hush analysis of its optical spectral properties.

Results

Neutral 3. **3** was prepared by acylating 2-oxa-3-azabicyclo-[2,2,2]oct-5-ene hydrochloride with **1**-COCl, followed by catalytic hydrogenation, a method similar to that used for the compounds previously studied.[1] Its X-ray crystal structure was obtained and the atom numbering shown in Figure 1 used (the atom positions in the line drawing shown are a projection of those in the crystal), where it may be seen that hydroxylamine units are unsymmetrically disposed with respect to the CO group. The N(1)O(2) hydroxylamine unit is s-cis (*Z*) to the C=O group and the N(2)O(3) units s-trans (*E*). The bond lengths and bond angles about the heteroatoms are shown in Figure 2. Close intramolecular nonbonded distances are O(1)O(2) (2.60 Å), O(3)N(1) (2.62 Å), and O(1)C(10) (2.74 Å), all significantly less than the ca. 2.9 Å van der Waals contact distance for these atoms. It will be noted that both nitrogens are substantially pyramidal, but the carbonyl carbon is planar [α(av) at C(13) is 120.0°]. α(av) at the *Z* hydroxylamine nitrogen N(1) is 112.7° ["70% pyramidalized" from α(av) = 120° for a planar atom toward the 109.5° for a tetrahedral one], while that at the *E* hydroxylamine nitrogen N(2) is 114.3° (54% pyramidalized). The direction of pyramidalization of the nitrogens is that which relieves the serious nonbonded steric

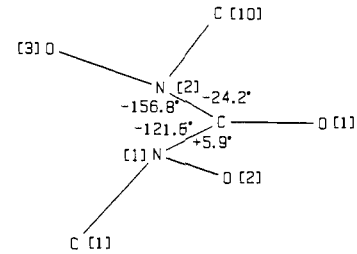

Figure 3. Projection of the atom positions about the heavy atoms of **3**.

Table I. PES and CV Data[a] for Some 3-Acyl-2-oxa-3-azabicyclo[2.2.2]octanes

compd	vIP, eV	$E^{\circ\prime}$(E_{pp}[b]), V
2[c]	8.53	1.52 (0.07)
4[c]	8.13	1.15 (0.07)
3	8.20	1.17 (0.10)

[a] Conditions: 2 mM in 0.1 M n-Bu_4NClO_4/CH_3CN, scan rate 0.2 V/s at a Pt electrode, reported vs saturated calomel reference electrode. [b] Difference between the oxidation and reduction peak potentials. [c] From ref 1.

interactions in this rather congested compound, as may be seen in Figure 3, in which only the atoms attached to the heteroatoms are shown for clarity, along with the dihedral angles the atoms attached to nitrogen make with the C=O group. Assuming that the nitrogen lone-pair axes lie along the bisector of the CNO angles in Newman projections down the N—C=O bonds, the dihedral angle between the more pyramidal *Z* hydroxylamine N(1) axis and the carbonyl carbon p orbital axis is 31.8°, while the flatter *E* hydroxylamine N(2) lone pair is perfectly aligned for conjugation with the carbonyl carbon p orbital axis (dihedral angle 0.1°). The N—C=O distances in **3** are similar, and both significantly longer than the 1.319 Å of the planar nitrogen *N*-formyl compound **2**.[1] The torsional twist angles of the bicyclo[2.2.2]octyl rings are substantially different. The *Z* alkoxyamine bicyclic ring resembles that of crystalline **2** (which is also *Z*) in being nearly untwisted [the C(1)N(1),O(2)C(4) dihedral angle is 4.1°], and the dihedral angle between the O(2) p orbital and the N(1) lone-pair axes is 28.4°. The *E* alkoxyamine bicyclic ring is significantly twisted [C(10)N(2),O(3)C(7) angle −23.4°], which decreases the destabilizing O(3) p orbital, N(2) lone-pair interaction (dihedral angle 45.6°).

Cation Radical 3. The gas-phase vertical ionization potential (vIP) measured by photoelectron spectroscopy (PES) and acetonitrile solution formal oxidation potential ($E^{\circ\prime}$) measured by cyclic voltammetry (CV), for **3** are compared with these data for its formyl- (**2**) and dimethylcarbamoyl- (**4**) substituted analogues

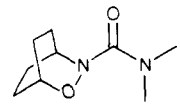

4

in Table I. The amide carbonyl substituted **1** derivatives **3** and **4** are both significantly easier to oxidize [8.3 (2) kcal/mol] than is the formyl-substituted compound **2**. Despite the possibility of extra stabilization for $\mathbf{3}^{\bullet+}$ by charge delocalization over both alkoxyamine units, $E^{\circ\prime}$ for **3** is no lower than that for **4**, which has only one alkoxyamine unit which clearly bears the majority of the spin in the cation radical from the ESR spectrum of $\mathbf{4}^{\bullet+}$. $\mathbf{4}^{\bullet+}$ has a nitrogen splitting of ~17.0 G, significantly higher than that of the formyl-substituted compound $\mathbf{2}^{\bullet+}$, which has a(N) of 13.43 G.[1] The ESR spectrum of $\mathbf{3}^{\bullet+}$ was studied by generating this cation by tris(2,4-dibromophenyl)aminium hexachloroantimonate (**5**; $E^{\circ\prime}$ = 1.70 V) oxidation of **3** in methylene chloride.

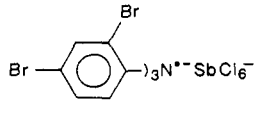

5

(1) Nelsen, S. F.; Thompson-Colon, J. A.; Kirste, B.; Rosenhouse, A.; Kaftory, M. *J. Am. Chem. Soc.* **1987**, *109*, 7128.

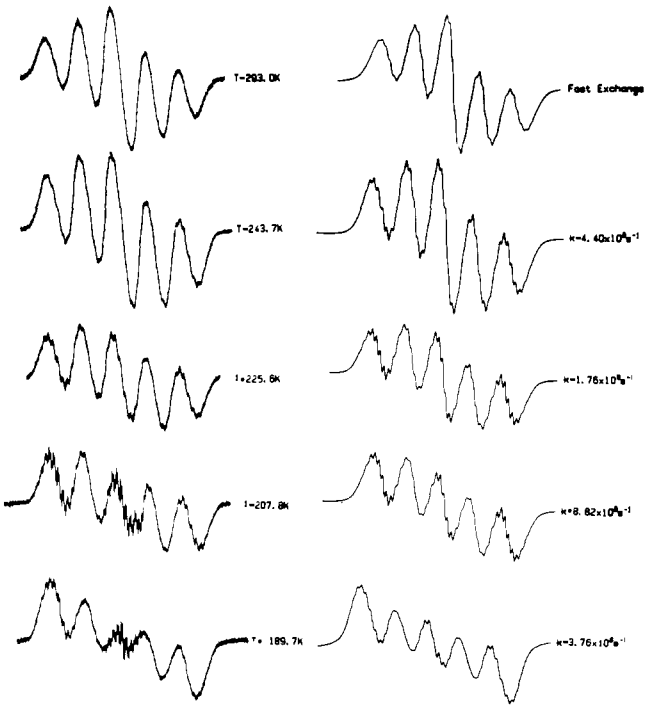

Figure 4. Experimental (left) and simulated (right) ESR spectra of $3^{\bullet+}$. The simulations use $a(2H) = 5.0$, $a(2H) = 2.4$, inherent line width 1.38 G, and the nitrogen splittings and exchange rate constants shown in Table II.

Table II. Best Fit Parameters for Simulation of the ESR Spectrum of $3^{\bullet+}$

T, °C	a(N), G	k_{th}, s^{-1}	$\Delta G^{\ddagger}_{th}$[a]
-83.5	18.0_6	$3.7_6 \times 10^8$	3.51 [11]
-65.4	18.3_1	$8.8_2 \times 10^8$	3.50 [7]
-47.6	18.3_8	$1.7_6 \times 10^9$	3.48 [8]
-29.5	18.5_6	$4.4_0 \times 10^9$	3.46 [13]

[a] Units, kilocalories per mole. Numbers in brackets are errors in the last place quoted estimated at the 95% confidence level. Activation parameters calculated from these data are $\Delta H^{\ddagger}_{th} = 3.7 \pm 0.7$ kcal/mol and $\Delta S^{\ddagger}_{th} = 0.9 \pm 3.4$ cal deg^{-1} mol^{-1}.

The half life of $3^{\bullet+}$ at room temperature under these conditions was estimated to be 1 h from the decrease of its ESR signal intensity; that for $4^{\bullet+}$ under the same conditions is ~10 min. The room-temperature ESR of $3^{\bullet+}$ exhibits five broad lines for two equivalent nitrogens, a(N) about 9.3_5 G. As for $4^{\bullet+}$, the proton splittings were not resolved. Decreasing the temperature causes fine structure to appear in the center and outer lines, and the relative intensity of the intermediate lines decreases, as expected for slowing the rate of electron transfer between the NO units of $3^{\bullet+}$. The ESR spectra of acylated **1** cation radicals for which

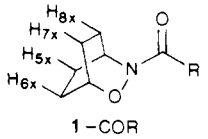

1-COR

good resolution was achieved exhibit two 2H splittings for the exo hydrogens, the larger (range 4.0–4.5 G) assigned to H(5x,8x), which increases as the nitrogen splitting increases when the acyl substituent at N(2) is changed, and the smaller (range 2.3–3.1) assigned to H(6x,7x), which decreases as the nitrogen splitting increases.[1] In addition, splittings under 1 G were resolved in favorable cases for H(5n,8n), H(1), and the hydrogens in the acyl substituent. For example $2^{\bullet+}$ shows a(H(5x,8x)) = 4.11, a(H(6x,7x)) = 2.35, a(H(5n,8n)) = 0.71, and a(H(1,CHO)) = 0.56 G.[1] The ESR spectrum of $3^{\bullet+}$ was simulated at various temperatures using $a(2H) = 5.0$ G, $a(2H) = 2.4$ G, and a line width of 1.38 G, adjusting for best visual fit varying a(N) and the rate constant for thermal electron transfer between two equivalent sites

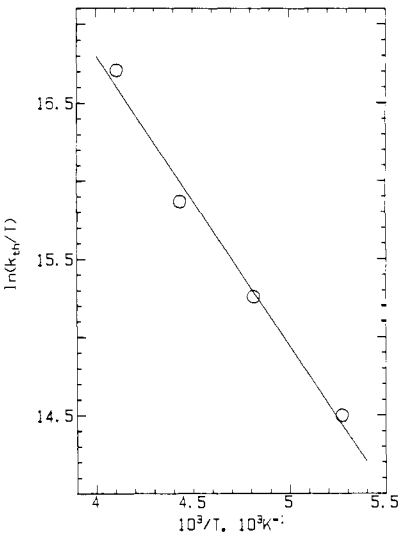

Figure 5. Eyring plot the data of Table II.

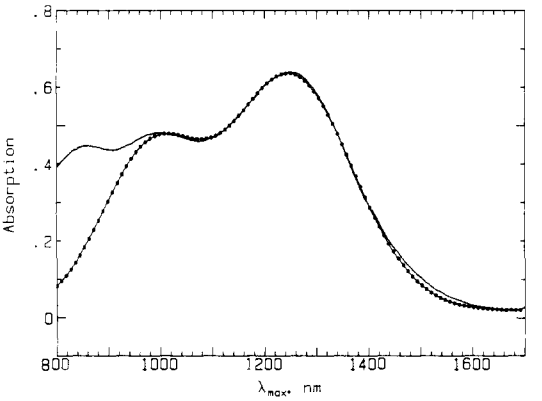

Figure 6. Near-IR spectrum of $3^{\bullet+}$ in CH_3CN, along with a Gaussian sum fit to the first two bands (λ_{max} = 1250 nm, $\nu_{1/2}$ = 280 nm, absorbance 0.61; λ_{max} = 980, $\nu_{1/2}$ 220 nm, absorbance 0.40). The solution was initially 0.98 mM in **5** and 6.1 mM in **3**.

(the two bicyclic rings), k_{th}. The experimental and simulated ESR spectra are compared in Figure 4, and the simulation parameters are listed in Table II. These numbers give the Eyring plot shown as Figure 5, which has a correlation coefficient of −0.994, and an extrapolated $\Delta G^{\ddagger}_{th}$ at 25 °C of 3.4 ± 0.3 kcal/mol.

The optical spectra of $3^{\bullet+}$ and $4^{\bullet+}$ in the UV and visible regions were examined by using electrolytic generation in acetonitrile containing 0.1 M tetrabutylammonium perchlorate to avoid interference problems from chemical oxidants. Neutral **4** shows a maximum at 255 nm (ϵ 2200 M^{-1} cm^{-1}), and increased absorption after partial oxidation (concentration of $4^{\bullet+}$ not known because decomposition is occurring) indicates maximums at ca. 230 and 390 nm for the cation radical. Neutral **3** has a maximum at 219 nm (ϵ 3600 M^{-1} cm^{-1}), and increased absorption was also observed both near the maximum of neutral **3** and near 400 nm; but in addition, $3^{\bullet+}$ exhibits three broad, overlapping near-IR bands. The spectrum in 0.1 M CH_3CN/tetrabutylammonium perchlorate shows maximums at 1250 (ϵ 630 M^{-1} cm^{-1}), 980 (410), and 855 (280) nm. The ϵ values were estimated by assuming a 100% yield of $3^{\bullet+}$ in the oxidation of an excess of **3** with a known amount of **5**. The near-IR spectrum of $3^{\bullet+}$ in acetonitrile generated by **5** oxidation is shown in Figure 6 along with a Gaussian sum fit of the two longer wavelength bands. The near-IR of $3^{\bullet+}$ was only studied at room temperature. The near-IR absorption for $3^{\bullet+}$ seems clearly to be associated with the presence of two NO groups in the molecule, as it is not observed for $4^{\bullet+}$. The solvent dependence of the longest wavelength maximum appears in Table III. **5** proved to be too unstable in DMSO to allow use of this solvent, and we were unable to get enough **3** to dissolve in ethyl carbonate to use it.

Table III. Solvent Effect on Near-IR Absorption Maximum of $3^{\bullet+}$ [a]

solvent	Marcus γ	λ_m, nm	E_{op} [b]
$CHCl_3$	0.266	1320	21.6_6
CH_2Cl_2	0.381	1305	21.9_2
$PhNO_2$	0.384	1300	22.0_0
PropC[c]	0.481	1280	22.3_4
CH_3CN	0.526	1260	22.7_0

[a] Generated by **5** oxidation. [b] Units, kilocalories per mole. [c] Propylene carbonate.

Discussion

Mixed-valence transition-metal complexes offer simplified controlled electron transfer systems in which the distance between the redox sites is fixed by ligands that bridge the metals. The relationship between their intervalence transfer (IT) optical absorption bands and thermal electron transfer properties was developed by Hush.[2] We shall only consider dimeric mixed-valence compounds in which the redox sites are formally identical, the seminal first example of which, **6**, was reported in 1969 by Creutz

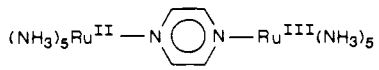

6

and Taube[3] and was followed by a blossoming of research in the area.[4]

Although the nature of the redox sites is obviously quite different in organic cation radicals and transition-metal mixed-valence complexes, $3^{\bullet+}$ does have formally identical physically separated sites for the hole and shares with metal complexes the spectral property of a solvent-sensitive near-IR band. We shall discuss its optical spectrum in terms of a classical Hush analysis. Robin and Day[5] classified mixed-valence metal compounds on the basis of the degree of resonance interaction between the metal centers: Class I is used for compounds having such firmly trapped valences that there is no resonance interaction and hence no intervalence transition, class II for compounds with trapped valences that have slight delocalization (this is the class to which Hush theory applies), and class III for fully delocalized systems without separate energy minimums for metal atoms in different oxidation states. Applying the Robin and Day classes to organic compounds, the cation radicals of bis(hydrazines) **7** and **8**[6] show no intervalence

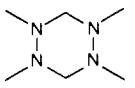

7

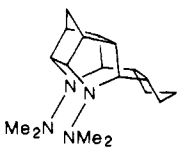

8

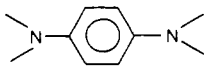

9

absorption[7] despite the fact that it ought to occur in the visible region, where sensitivity for its detection is high. We suggest that these bis(hydrazine) cation radicals should be considered class I organic cation radicals. Such large relaxation energies (energy difference between the vertical cation radical and the relaxed, adiabatic cation radical) occur upon electron loss from most hydrazines (approximately 1–1.5 eV)[8] that there is apparently no significant resonance interaction even when reduced and oxidized hydrazines are forced to lie close to each other in space. We are not aware of any example of an organometallic dimer mixed-valence class I complex and suspect that quite large relaxation energies upon electron loss are required for Class I behavior. Many examples of class III organic cation radicals are known, such as the cation radical of tetramethyl-*p*-phenylenediamine (**9**). $9^{\bullet+}$ could have different nitrogens, but instead clearly exists as the delocalized cation with equivalent nitrogen atoms. We do not doubt that many examples of class II organic cation radicals are also possible, but are not aware of a previous attempt to carry out a Hush analysis of one.

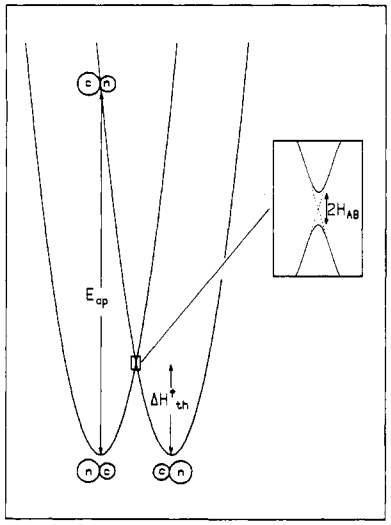

Figure 7. Hush diagram for a dimeric species with neutral and cation-radical centers.

Table IV. Comparison of λ_i and λ_o Values Obtained from eq 1–3 for Urea Cation Radical $3^{\bullet+}$ with Diruthenium Complexes **10–12**

compd	λ_i [a]	λ_o [a] (CH_3CN)	d, [b] Å
$3^{\bullet+}$	20.5	2.1	
10	16.2	5.8	6.9
11	16.8	12.3	11.1
12	17.8	13.1	13.2

[a] Units, kilocalories per mole. Entries for **10–12** are calculated (see ref 10) from the data of ref 9c, which lists 6.7, 12.5, and 16.1 for λ_o of **10–12**, respectively. [b] Estimated Ru,Ru distance (ref 9c).

According to Hush theory, the energy of the IT absorption band, E_{op}, corresponds to the energy for vertical ET between the sites, making the thermal ET barrier, which we shall call $\Delta H^{\ddagger}_{et}$ (Eyring rate theory is often not employed, but E_{op} is an enthalpy, not a free energy) one-quarter E_{op} because of the parabolic shape of energy wells (eq 1; see Figure 7 for a pictorial representation).

$$E_{op} = 4\Delta H^{\ddagger}_{et} \quad (1)$$

E_{op} (which is the same as the Marcus λ value for these systems) is separated into inner shell, λ_i (internal geometry reorganization), and outer shell, λ_o (solvent reorganization), terms (eq 2). This

$$E_{op} = \lambda_i + \lambda_o \quad (2)$$

solvent reorganization term is numerically calculated in eq 3.

$$\lambda_o = 332.4g(r,d)\gamma \quad (3)$$

$$g(r,d) = 1/r - 1/d \quad (4)$$

Equation 3 uses a dielectric continuum model with the distance parameter $g(r,d)$ (eq 4) which is calculated from r, the effective

(2) (a) Hush, N. S. *Trans. Faraday Soc.* **1961**, *57*, 557. (b) Allen, G. C.; Hush, N. S. *Prog. Inorg. Chem.* **1967**, *8*, 357. (c) Hush, N. S. *Ibid.* **1967**, *8*, 391. (d) Hush, N. S. *Electrochim. Acta* **1968**, *13*, 1005. (e) Hush, N. S. *Chem. Phys.* **1975**, *10*, 361.

(3) (a) Creutz, C.; Taube, H. *J. Am. Chem. Soc.* **1969**, *91*, 3988. (b) Creutz, C.; Taube, H. *Ibid.* **1973**, *95*, 1086.

(4) (a) Creutz, C. *Prog. Inorg. Chem.* **1983**, *30*, 1. (b) Cannon, R. D. *Electron Transfer Reactions*; Butterworths: London, 1980. (c) Meyer, T. J. *Acct. Chem. Res.* **1978**, *11*, 94. (d) Sullivan, B. P.; Curtis, J. C.; Kober, E. W.; Meyer, T. J. *Nouv. J. Chim.* **1980**, *4*, 643. (e) Taube, H. *Ann. N.Y. Acad. Sci.* **1978**, 481. (f) Meyer, T. J. *Ibid.* **1978**, 496.

(5) Robin, M. B.; Day, P. *Adv. Inorg. Radiochem.* **1967**, *10*, 247.

(6) (a) Nelsen, S. F.; Hintz, P. J.; Buschek, J. M.; Weisman, G. R. *J. Am. Chem. Soc.* **1975**, *97*, 4933. (b) Nelsen, S. F.; Willi, M. R.; Mellor, J. M.; Smith, N. M. *J. Org. Chem.* **1986**, *51*, 2081.

(7) Kim, Y., unpublished work.

(8) (a) Nelsen, S. F.; Blackstock, S. C.; Kim, Y. *J. Am. Chem. Soc.* **1987**, *109*, 677. (b) Nelsen, S. F.; Rumack, D. T.; Meot-Ner (Mautner), M. *Ibid.* **1987**, *109*, 1373. (c) Nelsen, S. F.; Rumack, D. T.; Meot-Ner (Mautner), M. *Ibid.* **1988**, *110*, 7945.

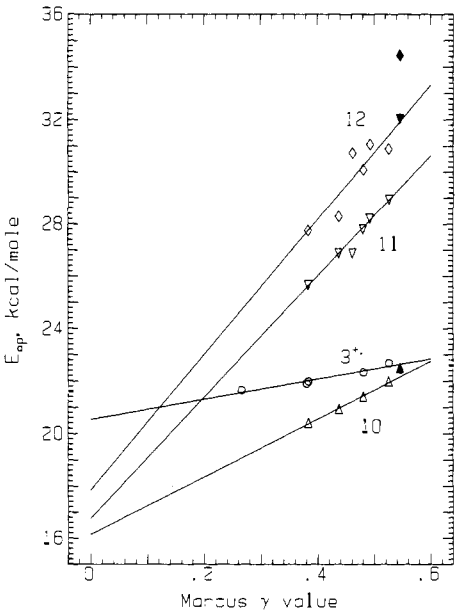

Figure 8. Comparison of Marcus–Hush plots for $3^{\bullet+}$ and **10–12**. The points measured in water are filled. The lines are linear regressions ignoring the water points, extrapolated to $\gamma = 0$, where E_{op} is λ_i.

radius of the localized charge represented as a sphere centered at the metal atom, and d, the distance between the centers of the metal atoms. The Marcus solvent parameter, γ, is defined in eq 5, where n is the refractive index of the solvent at the sodium D

$$\gamma = 1/n^2 - 1/\epsilon \qquad (5)$$

line and ϵ its dielectric constant. The constant quoted in eq 3 is that necessary to give λ_o in kilocalories per mol when the distances in $g(r,d)$ are in Å. Both the predicted linearity of E_{op} versus γ plots and the $1/d$ dependence are found experimentally.[4] These equations allow separation of the solvent reorganization (λ_o) from the internal geometry reorganization (λ_i) portion of E_{op} and allow evaluation of r from the d value, which is rather accurately known from the known geometry of the bridging ligand. These equations are commonly assumed to give accurate $\Delta H^{\ddagger}_{et}$ values, which are extremely difficult to determine experimentally for dimeric mixed-valence metal compounds.

Figure 8 shows a Marcus–Hush plot of E_{op} versus γ for $3^{\bullet+}$ (as the circles), along with plots of Meyer's series of class II ligand-bridged diruthenium bis(Bipy) chloride (L_3Ru) compounds[9] **10–12** for comparison, and Table IV shows some data derived for

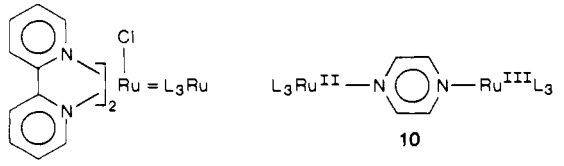

10

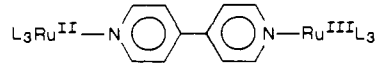

11

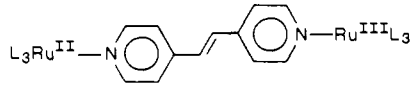

12

these four compounds by using eq 1–3. It will be noted that the E_{op} values for $3^{\bullet+}$ plot as well versus γ as those for **10–12**, and extrapolation to $\gamma = 0$ gives λ_i of 20.5 kcal/mol for $3^{\bullet+}$. This is of the order expected from previous work on acylated hydroxylamines. Deviations of $E^{\circ\prime}$ values for **2** and hydrazine **13**

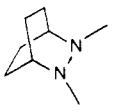

13

in $E^{\circ\prime}$ vs vIP plots from the line formed by compounds with small reorganization energies upon electron loss indicate that the internal relaxation energy for **3** is ~46% that of **13**.[1] The enthalpy of cation-radical relaxation, ΔH_r, for **13** has been measured at 23.3 kcal/mol in the gas phase.[8c] We have pointed out that ΔH_r is close to half of the Marcus λ_i value.[8a]

Despite the reasonable size of the λ_i value obtained from Figure 7, the sensitivity of E_{op} to changes in solvent polarity is far smaller for $3^{\bullet+}$ than it is for any of the diruthenium intervalence complexes.[10,11] For **10** and even **11**, the Marcus–Hush charge spheres interpenetrate. Powers and Meyer estimated r at about 6.0–6.4 Å, greater than $d/2$ for both compounds (Table IV).[9c] Neither d nor r is simply defined for an organic compound, but the charge spheres would be expected to interpenetrate even more for $3^{\bullet+}$, and the rationalization for eq 3 assumes that solvent is between spheres representing the charge centers. It does not seem surprising that the effect of solvent is substantially less than predicted by eq 3 and 4 (as it is for **10**).[10] There is little room for solvent between the bicyclic rings of $3^{\bullet+}$.

Hush[2] derived the relationship between near-IR band position, ν_{max}, and its minimum full width at half-height $\Delta\nu_{1/2}$, for symmetrical, homonuclear organometallic IT complexes shown as eq 6. Equation 6 has proven very useful in assigning mixed-valence

$$\Delta\nu_{1/2}(\text{cm}^{-1}) = 48.06(\nu_{max})^{1/2} \qquad (6)$$

dimers because Robin–Day class II compounds reliably show $\Delta\nu_{1/2}$ values slightly larger than the eq 6 prediction. On the basis of over 100 complexes, Creutz[4a] has stated that if the near-IR band is narrower than eq 6 predicts, the complex is class III. For example, the original Creutz–Taube dimer **6** shows $\Delta\nu_{1/2}$ of 1.4 $\times 10^3$ cm^{-1}, only 16% that of the eq 6 prediction, and complex **14** shows $\Delta\nu_{1/2}$ of 2.1 $\times 10^3$ cm^{-1}, 48% of the eq 6 prediction.[12]

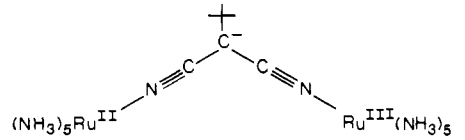

14

Both are assigned as class III complexes,[4a] are significantly more stable relative to their redox homovalent relatives than would be expected if resonance stabilization were not occurring, and do not exhibit the linear solvent sensitivity with γ characteristic of class II complexes.

(9) (a) Powers, M. J.; Salmon, D. J.; Callahan, R. W.; Meyer, T. J. *J. Am. Chem. Soc.* **1976**, *98*, 6731. (b) Callahan, R. W.; Keene, F. R.; Meyer, T. J.; Salmon, D. J. *Ibid.* **1977**, *99*, 1064. (c) Powers, M. J.; Meyer, T. J. *Ibid.* **1980**, *102*, 1289.

(10) The numbers in Table IV differ somewhat from those in ref 9, because we did not use the water data for any of the compounds in determining the lines for extrapolation to $\gamma = 0$. It is well established from intermolecular kinetics studies that γ values for water and other hydroxylic solvents are inappropriate ones for comparison of rates with those obtained in non-hydroxylic solvents.[11] The water point was used in determining the line for **10** and **12** but not **11** in ref 9c. Unfortunately the E_{op} value for **12** plotted in their Figure 1 is clearly not that obtained from the λ_m quoted in their Table IV. The correct value for **12** in water deviates as much as that for **11** (see our Figure 7). We believe it should be noted that eliminating the water points affects the agreement of the experimental data for **10–12** with Marcus–Hush theory in two ways. λ_i now appears to increase slightly with d; it should not. Agreement of the $\lambda_o(CH_3CN)$ values calculated by substituting Meyer's estimated d and r values[9c] into eq 4 and 3 with those obtained from the solvent variation study is substantially improved: λ_o values of 3.8 kcal/mol for **10** (34% too low relative to the solvent variation result, Table IV), 11.5 for **11** (7% too low), and 13.6 for **12** (4% too high). Agreement is excellent at larger d, and as Meyer and co-workers point out, good agreement is not really expected at small d.[9c]

(11) Grampp, G.; Jaenicke, W. *Ber. Bunsenges. Phys. Chem.* **1984**, *88*, 325, 335.

(12) Krentzien, H.; Taube, H. *J. Am. Chem. Soc.* **1976**, *98*, 6379.

$3^{\bullet+}$ shows anomalous near-IR absorption compared to organometallic complexes in that three partially resolved bands that decrease in ϵ as the wavelength becomes shorter are observed. The longest wavelength band used in the analysis above is obviously too narrow to fit eq 6. It is centered at 1250 nm (8×10^3 cm^{-1}) in CH_3CN/0.1 M n-Bu_4ClO_4 and is simulated (Figure 6) as a Gaussian peak with full width of 280 nm ($\Delta\nu_{1/2} = 1.8 \times 10^3$ cm^{-1}) while the eq 6 prediction is 4.3×10^3 cm^{-1}. Nevertheless, $3^{\bullet+}$ experimentally is not a delocalized, "class III" cation radical, but has its hole instantaneously centered on one of its NO units. As noted in Results, **3** is thermodynamically no easier to oxidize than is **2**, which only has one hydroxylamine unit to bear the spin and charge; the dynamic ESR spectrum of $3^{\bullet+}$ is consistent with spin transfer between the two units becoming slow at low temperature, and the solvent dependence for the near-IR band of $3^{\bullet+}$ is consistent with this localization. Furthermore, a substantial relaxation enthalpy is associated with electron removal from a hydroxylamine, and although ROR'N,C=O conjugation is large in the neutral compound, it is essentially lacking in the cation radical.[1] Both nitrogens must share conjugation with the C=O group in neutral **3**, but in the cation radical, the reduced nitrogen ought to be able to increase its N,C=O resonance interaction, and the spin localize at the other NO unit, accompanied by a 90° twist about one N–(C=O) bond. Semiempirical MO calculations do predict such localization in urea cation radicals, and it has been observed experimentally for matrix-isolated tetramethylurea cation radical.[13] Perhaps one should consider not just the longest wavelength band but all three near-IR bands in comparing to the Hush band width eq 6. The total width of the three near-IR bands of $3^{\bullet+}$ at half-height of the maximum is $\sim 5.7 \times 10^3$ cm^{-1}, rather larger than the usual increase over the eq 6 prediction that is observed for bimetallic intervalence dimers. We do not know why the near-IR region of $3^{\bullet+}$ shows three narrow bands instead of the broad band typical for organometallic compounds, or why the overall shape of the three bands is so non-Gaussian (the largest ϵ component comes at the longest wavelength). We do not doubt that $3^{\bullet+}$ has substantial hole localization in one bicyclooctyl ring, and that the near-IR absorptions observed are connected with charge transfer.[14]

Dynamic ESR experiments conducted over a 54 °C range gave estimates of $\Delta G^{\ddagger}_{th}$ (25 °C) of 3.4 (3) kcal/mol and $\Delta H^{\ddagger}_{th}$ of 3.7 (7) kcal/mol in methylene chloride. This thermal ET barrier is less than the 5.5 kcal/mol $E_{op}/4$ value in the same solvent. Hush pointed out that class II complexes must have some resonance interaction, H_{AB}, to allow crossing between the energy surfaces of the two largely localized ET forms (see Figure 7 for a pictorial representation). Hush uses eq 7 to replace eq 1 when H_{AB} is

$$E_{th} = E_{op}/4 - H_{AB} + (H_{AB})^2/E_{op} \quad (7)$$

significant compared to $E_{op}/4$. Using E_{th} as 3.4–3.7 kcal/mol, eq 7 gives H_{AB} in the range 2.35–2.2 kcal/mol. Hush uses the fractional delocalization at the transition state for ET, α^2, calculated from eq 8 with eq 9 to estimate the size of H_{AB} for

$$\alpha^2 = (4.2 \times 10^{-4})\epsilon_{max}\Delta\nu_{1/2}/\nu_{max}d^2 \quad (8)$$

$$H_{AB} = \alpha\nu_{max} \quad (9)$$

binuclear metal IT complexes. A difficulty in applying these equations to organic systems is that the structures do not have a clear single-charge center to allow definition of d (we note that this problem also exists in attenuated form for organometallics, and that Meyer's group ended up changing d from the Ru,Ru distance in interpretation of the effect of d on the optical properties of **10–12**).[9c] Using the shortest conceivable distance for $3^{\bullet+}$, the 2.33 Å NN distance, gives α^2 of 0.011, while it is 0.006 employing the 3.3 Å average of the NN and OO distances in the perpendicular NO geometry expected for $3^{\bullet+}$, when the observed 1.8×10^3 cm^{-1} band width of the 1250-nm (8.0×10^3 cm^{-1}) band is employed. Equation 8 predicts under 1% delocalization for $3^{\bullet+}$ if these assumptions are made. If the 5.7×10^3 cm^{-1} band width embracing all three observed near-IR bands is employed, α^2 is still under 2% if d is over 3.3 Å (it is 0.017 at d = 3.3 Å). With eq 9, an α^2 of 0.01 is consistent with the ca. 2.3 kcal/mol H_{AB} value that fits the dynamic ESR, E_{op} comparison using eq 7. Although **3** is no easier to oxidize than **4**, we do not believe this rules out a 2.3 kcal/mol (0.1 eV) value of H_{AB} for $3^{\bullet+}$. $E^{\circ\prime}$ is determined by the energy gap between the neutral compound and its relaxed cation radical, while H_{AB} refers to resonance delocalization at the transition state for electron transfer. For a compound with a rather large relaxation enthalpy, such as **3**, resonance delocalization in the relaxed cation radical and at the transition state for ET should be substantially different.

Conclusion

The bis(N-alkoxyurea) derivative **3** gives a cation radical that is usefully considered an organic analogue of class II bimetallic IT complexes. $3^{\bullet+}$ shows near-IR absorption corresponding to charge transfer, and the solvent effect on E_{op} using a standard Marcus–Hush solvent polarity change analysis produces a large λ_i value consistent with expectation based upon independently determined relaxation energies of N-acylmonoalkoxylamine cation radicals. The thermal barrier to ET in $3^{\bullet+}$, ca. 3.5 kcal/mol, is significantly less than $E_{op}/4$, but is consistent with a ~2 kcal/mol lowering of the ET barrier caused by delocalization between the hydroxylamine centers (which are close in space) at the ET transition state.

We suggest that the principal reasons for interest in dimeric organic cation radicals in the context of Marcus–Hush theory are that it is far easier to measure thermal barriers for them because of more favorable magnetic properties of first-row elements than transition metals and because significant structural variations are easier to achieve. Much is now known about how ΔH_r varies with structure for nitrogen-containing cation radicals,[8] and cation radicals exhibiting both class I and class III behavior are known. We hope to be able to probe the regions of transition in behavior and, most importantly, to explore the effects of changing distance between the charge-bearing centers. Unfortunately, preliminary work not worth presenting in detail has shown that acylated **1** derivatives are not the compounds to use for these studies. $3^{\bullet+}$ proved to be uniquely long-lived in solution, and analogues with its carbonyl group replaced by oxalyl, terephthalyl, and hexahydroterephthalyl units all proved to lack the lifetime necessary to make the measurements reported here for $3^{\bullet+}$.[7] We are now surveying for more robust charge-bearing units with the desired intermediate ΔH_r values to use in studies that vary the distance between the units.

Experimental Section

Carbonylbis[3-(2-oxa-3-azabicyclo[2.2.2]octane)] (3). A mixture of 0.30 g (1.88 mmol) of 2-oxa-3-azabicyclo[2.2.2]oct-5-ene hydrochloride and 0.35 g (1.99 mmol) of **1**-COCl in 3 mL of methylene chloride was stirred for 12 h at room temperature and extracted with brine, and the aqueous layer was extracted twice with 5-mL portions of ether. The organic layers were dried over magnesium sulfate and concentrated to give 0.26 g (56%) of monounsaturated **3**, which was hydrogenated in ethyl acetate over 10% Pd/C, giving **3** in 97% crude yield. The product was filtered through Celite, which was washed with methylene chloride. After concentration, the crude material was washed through a pad of neutral alumina (activity grade I) with 1:1 ethyl acetate/hexane, concentrated, and recrystallized (ethyl acetate/hexane), giving **3**, mp 160–161 °C. Empirical formula was established by high-resolution mass spectroscopy: ^{1}H NMR ($CDCl_3$) δ 4.13 (br s, 4 H), 2.18 (m, 8 H), 1.66 (m, 8 H); ^{13}C NMR ($CDCl_3$) δ 71.5 (CH), 49.0 (CH), 24.8 (CH2), 23.3 (CH2); IR ($CHCl_3$) 1565 cm^{-1}.

Crystallography of 3: $C_{13}H_{20}N_2O_3$; orthorhombic space group $Aba2$; a = 10.247 (5), b = 21.109 (11), c = 11.520 (6) Å; the calculated density for z = 8 is 1.344 g/cm^3. The crystal structure was solved by MULTAN80[14] and refined by SHELX.[15] The refinement was performed in a full-matrix

(13) Qin, X.-Z.; Pentecost, T. C.; Wang, J. T.; Williams, F. *J. Chem. Soc., Chem. Commun.* **1987**, 450.

(14) A reviewer suggested that vibronic coupling might be the cause of the multiple bands in the near-IR of $3^{\bullet+}$, which would make the classical Hush analysis inadequate. As pointed out in the next paragraph, the classical analysis does not seem very adequate. The 1250 and 980 near-IR bands of $3^{\bullet+}$ are separated by ~2200 cm^{-1}. The IR spectrum of solutions containing $3^{\bullet+}$ show medium intensity bands near 1780 and 1610 cm^{-1}, but only very weak absorption near 2000 cm^{-1}.

Table V. Heavy-Atom Coordinates ($\times 10^4$) and U_{eq} {$^1/_3$ Trace U ($Å^2 \times 10^3$)} for **3**

atom	X	Y	Z	U_{eq}
O(1)	-200 (4)	2124 (2)	1708	58 (1)
O(2)	-2263 (4)	1547 (3)	2495 (6)	70 (1)
O(3)	1309 (4)	782 (2)	2855 (5)	46 (1)
N(1)	-998 (4)	1319 (2)	2854 (6)	43 (1)
N(2)	1232 (4)	1443 (2)	2527 (6)	38 (1)
C(1)	-945 (5)	1261 (3)	4143 (6)	45 (1)
C(2)	-2015 (6)	809 (3)	4517 (8)	58 (1)
C(3)	-3327 (8)	1095 (4)	4174 (9)	85 (2)
C(4)	-3064 (5)	1692 (3)	3459 (7)	53 (1)
C(5)	-2439 (8)	2172 (3)	4232 (8)	66 (2)
C(6)	-1156 (6)	1909 (3)	4689 (7)	52 (1)
C(7)	1964 (6)	427 (3)	1916 (6)	48 (1)
C(8)	3408 (6)	582 (4)	2042 (8)	61 (2)
C(9)	3515 (6)	1313 (4)	2091 (7)	54 (2)
C(10)	2253 (5)	1603 (2)	1660 (6)	40 (1)
C(11)	1869 (5)	1303 (3)	500 (6)	44 (1)
C(12)	1409 (6)	626 (3)	768 (7)	52 (1)
C(13)	-23 (5)	1664 (2)	2315 (6)	38 (1)

least-squares procedure with H-atom positions riding on their bonded heavy atoms. The agreement factors are $R = 0.056$ and $R_w = 0.069$ for 995 observed reflections [$F_o > 1.5\sigma(F_o)$] (out of 1096 measured unique reflections). {$w = 0.3782/[\sigma^2(F_o) + 0.0194F^2]$}. The heavy-atom atomic coordinates and U_{eq} data for **3** appear in Table V. Hydrogen atom coordinates, bond length and bond angle tables, a stereoscopic view, crystal-packing diagram, and anisotropic displacement parameters are included in the supplementary material.

Near-IR spectra were recorded on a Cary 170 using 1-cm quartz cells. Solvents were percolated through a column of activated basic alumina or 4A molecular sieves (propylene carbonate) before use to remove hydroxylic impurities and deaerated with a stream of nitrogen.

ESR and PE spectra and cyclic voltammetry experiments were carried out as previously described.[1] The dynamic ESR program of Heinzer was employed.[16]

Acknowledgment. We thank the NIH for partial financial support under Grant GM-29549. We thank Prof. A. B. Ellis for the use of the near-IR instrument.

Registry No. 1, 110589-99-6; **3**, 119336-12-8; **3**$^{\bullet+}$, 119336-14-0; **3** monounsaturated, 119336-13-9; **4**$^{\bullet+}$, 110590-21-1; **10**, 59978-63-1; **11**, 61260-90-0; **12**, 71631-54-4; 2-oxa-3-azabicyclo[2.2.2]oct-5-ene hydrochloride, 56239-25-9.

Supplementary Material Available: Stereoviews of the structure of **3** and its crystal packing, as well as tables of its atomic coordinates, atomic displacement factors, and bond lengths and angles, and plots of the PE spectra of **3** and **4** (7 pages). Ordering information is given on any current masthead page.

(15) Main, P.; Fiske, S. J.; Hull, S. E.; Lessinger, L.; Germain, G.; Declercq, S. P.; Woolfson, M. M. *MULTAN80, A System of Computer Programs for the Automatic Solution of Crystal Structures from X-Ray Diffraction Data*; Universities of York, England, and Louvain, Belgium, 1980.

(16) Sheldrick, G. M. *SHELX, Program for Crystal Structure Determination*; University of Cambridge, Cambridge, UK, 1976.

(17) Heinzer, J. *Quantum Chemistry Program Exchange* **1972**, *No. 209*.

Surface-Enhanced Resonance Raman and Electrochemical Investigation of Glucose Oxidase Catalysis at a Silver Electrode

Randall E. Holt and Therese M. Cotton*

Contribution from the Department of Chemistry, University of Nebraska—Lincoln, Lincoln, Nebraska 68588-0304. *Received August 8, 1988. Revised Manuscript Received November 22, 1988*

Abstract: Combined electrochemical and surface-enhanced resonance Raman scattering (SERRS) were used to investigate the non-Nernstian response of a Ag electrode to glucose oxidase (GO) activity. Square-wave voltammetry measurements indicated that AgO_2 was formed from the reaction of H_2O_2, a product of the enzymatic reaction, with the Ag surface. Dissolution of the oxide layer, in turn, generates sufficient Ag ion to form a flavin-Ag^+ complex. The formation of this complex was proven by a comparison of SERRS spectra obtained under a number of different conditions with the resonance Raman (RR) spectrum of the chemically prepared complex. A mechanism incorporating the electrochemical and SERRS results is proposed. The results demonstrate the potential of in situ SERRS for monitoring electrode surface reactions involving biomolecules. Furthermore, the results caution against the use of Ag (or other reactive materials) as electrodes for electrochemical studies or sensor devices involving GO catalysis.

I. Introduction

In the present study, in situ surface-enhanced resonance Raman scattering (SERRS) spectroscopy was used to provide structural information regarding the non-Nernstian, potentiometric response of a Ag electrode to glucose oxidase (GO) activity. The SERRS results, in combination with electrochemical measurements, have suggested a plausible mechanism for the potentiometric behavior that involves several reactions at the electrode surface.

SERRS has already been demonstrated to be a powerful technique for the study of chromophore-containing systems. These include a variety of biologically important molecules, such as heme-containing proteins,[1] porphyrins,[2] and more highly organized systems such as photosynthetic reaction centers[3] and membrane preparations from green plants[4] and photosynthetic bacteria.[5] The strength of SERRS lies in its combined surface and resonance

* Author to whom correspondence should be addressed.

(1) (a) Hildebrandt, P.; Stockburger, M. In *Spectroscopy of Biomolecules*; Alix, A. J. P., Bernard, L., Manfait, M., Eds.; Wiley: New York, 1985; pp 25-30. Hildebrandt, P.; Stockburger, M. *J. Phys. Chem.* **1986**, *90*, 6017. Hildebrandt, P.; Greinert, R.; Stier, A.; Stockburger, M.; Taniguchi, H. *FEBS Lett.* **1988**, *227*, 76-80. (b) Cotton, T. M.; Schultz, S. G.; Van Duyne, R. P. *J. Am. Chem. Soc.* **1980**, *102*, 7960-7962. (c) Cotton, T. M.; Timkovich, R.; Cork, M. S. *FEBS Lett.* **1981**, *133*, 39-44. (d) Smulevich, G.; Spiro, T. G. *J. Phys. Chem.* **1985**, *89*, 5168-5173. (e) Niki, K.; Kawasaki, Y.; Kimura, Y.; Higuchi, Y.; Yasuoka, N. *Langmuir* **1988**, *3*, 982-986. (f) deGroot, J.; Hester, R. E.; Kaminaka, S.; Kitagawa, T. *J. Phys. Chem.* **1988**, *92*, 2044-2048. deGroot, J.; Hester, R. E. *J. Phys. Chem.* **1987**, *91*, 1693-1696.

(2) Cotton, T. M.; Schultz, S. G.; Van Duyne, R. P. *J. Am. Chem. Soc.* **1982**, *104*, 6528-6532.

(3) Cotton, T. M.; Van Duyne, R. P. *FEBS Lett.* **1982**, *147*, 81-84.

0002-7863/89/1511-2815$01.50/0